

Numerical simulation of orbiting black holes

Bernd Brügmann, Wolfgang Tichy, Nina Jansen

Center for Gravitational Physics and Geometry and Center for Gravitational Wave Physics

Penn State University, University Park, PA 16802

(Dated: December 26, 2003)

We present numerical simulations of binary black hole systems, which for the first time last for about one orbital period for close but still separate black holes as indicated by the absence of a common apparent horizon. An important part of the method is the construction of commoving coordinates in which both the angular and radial motion is minimized through a dynamically adjusted shift condition. We use fixed mesh refinement for computational efficiency.

PACS numbers: 04.25.Dm, 04.30.Db, 95.30.Sf Preprint number: CGPG-03/12-3

One of the fundamental problems of general relativity is the two body problem of black holes in a binary orbit. Since in general relativity two orbiting bodies emit gravitational waves that carry away energy and momentum from the system, the two black holes spiral inward and eventually merge. Gravitational waves from black hole mergers are expected to be among the primary sources for gravitational wave astronomy [1, 2].

The last few orbits of a black hole binary fall into the strongly dynamic and non-linear regime of general relativity, and we therefore turn to numerical simulations to solve the full Einstein equations. Numerical relativity has seen many advances in recent years, but so far it has not been possible to simulate even a single binary black hole orbit. The first 3d simulation of a Schwarzschild black hole was performed in 1995 [3]. In [4], the first 3d simulation of spinning and moving black holes in a “grazing collision” was presented. The black holes start very close to each other inside the innermost stable circular orbit (ISCO). The apparent horizon (AH) initially has two components that subsequently merge. Grazing collisions have been studied numerically with moving regions of black hole excision [5], and without excision in the puncture evolution method [4, 6], where the punctures that correspond to the inner asymptotically flat ends of the black holes do not move. These simulations cover only a short time interval around the merger of the AHs of the black holes. The longest evolution time with convergence in the extracted waves was about $30M$ (where M is the total mass) [6], and the simulations become unstable and crash not much later. The usefulness of these methods can be extended by providing an interface to a perturbative, which allows the extraction of complete wave forms even when the black holes start their plunge at a larger separation near the ISCO [7, 8, 9], but again the interval of evolution with the full field equations reaches not more than about $15M$. While the technology to perform merger simulations has been steadily progressing, in typical simulations the evolution time before merger is less than $50M$ [10]. An open issue is therefore to find methods that allow longer lasting evolutions of two black holes before they merge, ideally allowing evolution times on the order of one or more orbital periods.

In this paper we present results for a new method to

choose commoving coordinates that makes it possible to evolve two black holes for about one orbital period for the first time. The black holes start out close to but well outside the ISCO, and the AHs do not merge before one orbital period has passed. Since there are many different choices for the various components of a numerical relativity simulation that crucially affect its quality, we will first describe each one of them in sufficient detail to establish our basic framework. We will then discuss the major new aspect of our method, the construction of commoving coordinates, and discuss our numerical results.

As initial data we choose puncture data [11] for two equal mass black holes without spin on a quasi-circular orbit based on an approximate helical Killing vector [12, 13]. Each configuration is determined by the coordinate distance ρ_0 of the punctures from the origin. We focus on $\rho_0 = 3.0M$, where M is the total ADM (Arnowitt-Deser-Misner) mass at the punctures. For $\rho_0 = 3.0M$, the ADM mass at infinity is $0.98461M$, the bare mass of one puncture is $0.47656M$, the size of the linear momentum of the individual black holes is $0.13808M$, the angular velocity is $0.054988/M$, and the orbital period is $T = 114M$. For comparison, post-Newtonian methods and the thin-sandwich approach find the ISCO in the neighborhood of $T = 65M$ [14], which translates to about $\rho_0 = 1.9M$ in our method. The effective potential method locates the ISCO near $\rho_0 = 1.1M$, $T = 35M$ [15, 16]. The specification of the initial data is completed by setting the lapse to unity and the shift to an initial value for commoving coordinates that we discuss below.

As evolution system we use the modified version of the Baumgarte-Shapiro-Shibata-Nakamura (BSSN) system that is described in detail in [17]. At the outer boundary we impose a radiative boundary condition [17] (we did not implement the monopole term). The black holes are handled by introducing a time independent excision boundary according to the “simple excision” method described in [18], with a generalization from cubical to spherical excision regions. We also perform control runs without excision using the puncture evolution method [4, 17], which typically do not last as long as the excision runs, but which allow us to check the excision method.

As coordinate conditions we use the dynamic gauge conditions that proved to be successful for single black

hole runs with and without excision [17, 18, 19] and for head-on collisions [17]. For the lapse we choose “1+log” slicing without explicit shift dependence, and for the shift we use a particular version of the “Gamma driver” condition:

$$\partial_t \alpha = -2\alpha K \psi^m, \quad (1)$$

$$\partial_t \beta^i = \frac{3}{4} \alpha^p \psi^{-n} B^i, \quad \partial_t B^i = \partial_t \tilde{\Gamma}^i - \eta B^i, \quad (2)$$

where α is the lapse, β^i is the shift, B^i is its first derivative, K is the trace of the extrinsic curvature, $\tilde{\Gamma}^i$ is the contracted conformal Christoffel symbol of BSSN, and ψ is the time independent conformal factor of Brill-Lindquist data. After some experimentation we settled for our binary runs on $m = 4$, which helps mimic the singularity avoidance of maximal slicing for puncture runs, and for the shift we set $n = 2$ and $p = 1$. These parameters are not necessarily optimal for merged black holes. We picked $\eta = 2/M$, which is adapted to long term stability of a single black hole of mass M , but close to the individual black holes the effective mass is $M/2$. Larger values of η give somewhat longer runs but do not have a major effect.

One important point to be made about the gauge conditions (1)-(2) is that although they work well for black holes without linear momentum, they do not impose corotating or commoving coordinates. Moving the black hole excision region is showing a lot of promise, e.g. [20], but here we attempt to minimize the dynamics around black holes at fixed coordinate positions by modifying the shift condition. In [10], approximate stationarity is achieved by adding a time independent corotation shift. However, for orbiting black holes we have to maintain stationarity over significantly longer time intervals.

The method that we have developed as a first step toward long term commoving coordinates is based on the shift vector

$$\beta_{com}^i = \psi^{-q} (A_1 \omega(-y, x, 0)^i - A_2 \dot{r}(x, y, 0)^i). \quad (3)$$

We have introduced Cartesian coordinates x , y , and z , with $\rho = (x^2 + y^2)^{1/2}$, and $r = (\rho^2 + z^2)^{1/2}$. Ignoring the factor ψ^{-q} , the first term is a rotation about the z -axis with angular velocity $A_1 \omega \rho$, and the second term is a radial motion with radial velocity $A_2 \dot{r} \rho$. Clearly, for two point particles on an inspiraling orbit this shift can cancel the dynamics of the point particles completely. For two orbiting black holes we can only compensate some aspects of the global motion, similar to balancing the bulk motion of two stars, with some dynamics remaining in the metric field.

For the runs reported below we have set $q = 3$, because this results in the natural fall off of the shift near punctures [17], and we use the same value with excision. The prefactor A_1 can be used to attenuate the angular shift for large r , which simplifies the outer boundary and the analysis at large r at the cost of introducing additional differential rotation, but for now we work with

$A_1 = 1$. Since ψ^{-3} tends to 1 for $r \rightarrow \infty$, the shift corresponds to a rigid rotation for large r , in particular the coordinate motion becomes superluminal beyond a light cylinder. For the radial shift we attenuate with $A_2 = (c^2 + 1)^s / [\rho_0 (c^2 + \rho^2 / \rho_0^2)^s]$, which is constructed such that at the initial radial distance ρ_0 to the black holes the norm of $A_2(x, y, 0)^i$ is unity, at the origin the norm is zero, for large ρ the fall-off is controlled by s , and the shape of the attenuation can be adjusted with c . We set $c = 1$ and $s = 2$.

Furthermore, to evolve for one orbital time scale it was necessary to introduce a dynamic control mechanism that adjusts the angular velocity $\omega(t)$ and radial velocity $\dot{r}(t)$. For simplicity we track the location and shape of the lapse α at the excision boundary by computing its “center of mass”, while for puncture runs we track the minimum of a parabola near the puncture. This defines a vector $a^i(t)$ measuring the asymmetry in the lapse that points from the center of the excision region (from the puncture) in the direction into which the lapse profile has moved off-center. We compute a correction $\Delta \beta^i$ to the shift at finite intervals Δt according to

$$\Delta \beta^i / \Delta t = -\gamma_{damp} \partial_t a^i(t) - k_{drive} (a^i(t) - a_0^i), \quad (4)$$

which defines a damped harmonic oscillator about position a_0^i . In our case, useful values for the coefficients are $k_{drive} = 0.2/M$ for the restoring force into the direction of the center and $\gamma_{damp} = 5$ for the damping force opposite to the tangent vector to the orbit of $a^i(t)$.

The evolution of the shift proceeds as follows. We initialize the shift according to (3), for example with $\omega = 0.88\Omega$ and $\dot{r} = 0$ for $\rho_0 = 3M$, where Ω is the angular velocity at infinity defined by the initial data. Note that close to the black holes a correction to Ω is necessary but not unexpected. We then evolve for a certain time interval, say $5M$, until lapse and shift have gone through their first rapid evolution to adjust themselves to the presence of the black holes. Every $\Delta t = 2M$ we update ω and \dot{r} and correct β^i according to (4), but for simplicity we leave its time derivative B^i unchanged.

We generalize the radiative boundary condition to a rigidly rotating frame, taking into account that the scalar wave propagation no longer happens along the radial direction, and that tensor components have to be rotated to the new frame. For a vector f^i the result is

$$\partial_t f^i = \beta^k f_{,k}^i - f^k \beta_{,k}^i - v \frac{x^k}{r} (f^i - f_\infty^i)_{,k} - \frac{f^i - f_\infty^i}{r}, \quad (5)$$

where v is the wave speed, and f_∞^i is the value of f^i at infinity. We have experimented with cubical and spherical outer boundaries, where the latter is expected to have less problems with a global rotation. A superluminal shift does not create a problem in our runs with the outer boundary at $24M$, $48M$, or $96M$, since we can lower the Courant factor in the outer regions of our fixed mesh refinement grid, which we describe below, by switching from Berger-Oliger time stepping to uniform time steps.

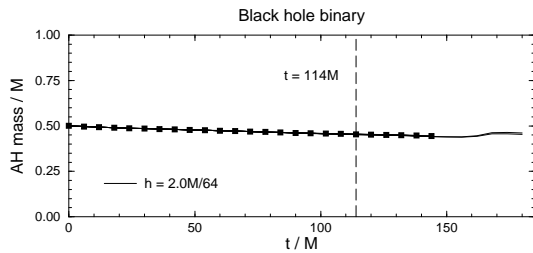


FIG. 1: Evolution of the AH mass for the black hole binary with $\rho_0 = 3.0M$. The evolution lasts longer than one orbital period of $114M$ defined by the initial data. The squares mark a run with 7 nested levels with coarsest resolution $2M$ and finest resolution $h = 0.03125M$, and with the spherical outer boundary at about $48M$, which crashes around $145M$. Also plotted are results from seven control runs with the outer boundary at $24M$ and $96M$, with a cubical outer boundary, and with the AH extracted on a coarser grid to check its convergence. There is little difference in the results, except that the runs with the boundary at $24M$ last somewhat longer.

All evolutions are carried out with a new version of the BAM code (“bi-functional adaptive mesh”) [21], which is built around an oct-tree, cell-centered adaptive mesh kernel that currently is functional for fixed mesh refinements (FMR) without parallelization. Adaptive mesh refinement (AMR) was made famous in numerical relativity by Choptuik’s work on critical collapse [22], and especially in 3d it can offer enormous savings over conventional unigrid codes. However, while the basic technical problem of writing AMR codes has been solved many times, see e.g. [23] for an overview and [24, 25, 26, 27] for some recent applications in numerical relativity, there have been only a handful of examples for the full 3d Einstein equations and the evolution of one [28, 29, 30] or two [4] black holes. The FMR technique with nested boxes introduced in [28] was essential for the feasibility of the first 3d grazing collision [4].

One aspect of the present paper is that we demonstrate that FMR can work successfully even for black holes in an orbital configuration. Our standard configuration consists of nested Cartesian boxes (where for black hole binaries with equal mass and no spin we only have to store one quadrant of the global domain). BAM’s Berger-Oliger FMR algorithm uses third order polynomial interpolation in space and second order polynomial interpolation in time, following essentially the recipe of [4, 28]. Note that the grazing collision in [4] showed growing constraint violations at the refinement boundaries, although the runs failed due to slice stretching independently of whether FMR or unigrid runs are performed. The main missing feature was a reasonably stable unigrid code with minimal slice stretching, which is now available for example in the form of BSSN with dynamic gauge as discussed above. An important detail of this setup is the use of the iterative Crank-Nicolson method for a method of lines time integration, which requires boundary conditions at a temporary, intermediate time level (as would Runge-

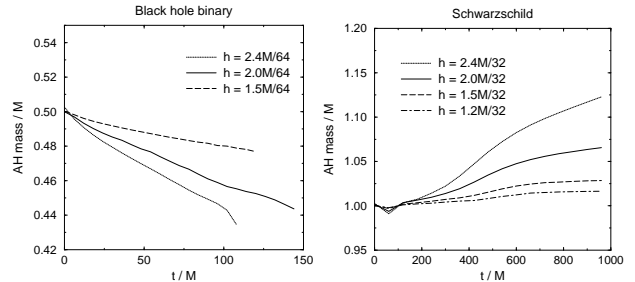


FIG. 2: Convergence in the AH mass. The panel on the left shows results for the black hole binary. The number and size of the refinement levels was not changed but the overall resolution was rescaled by a constant factor. There is a linear downward drift in the mass which becomes smaller with increasing resolution. The panel on the right shows convergence for a Schwarzschild black hole of mass $1M$ evolved in an octant to about $1000M$ with the same options except that commoving coordinates are turned off.

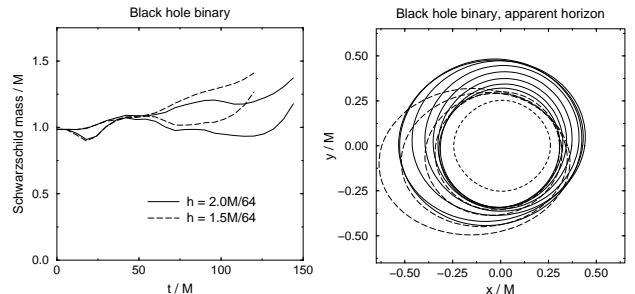


FIG. 3: Mass at large radius and coordinate location of the AH for the black hole binary, indicating current limitations. On the left, the mass at infinity is estimated on a sphere of radius $20M$ assuming a Schwarzschild background, showing fluctuations of about 20% to 40%. The lower and upper lines for a given resolution correspond to a cubical outer boundary at $24M$ and $48M$, respectively. On the right, the coordinate location of the AH around one of the black holes in the x - y plane is shown every $12M$ for a typical run. The AH starts as the smallest circle (dashed) in the center, quickly moves out to the largest circle within $5M$ of evolution while the gauge adjusts itself near the black hole, slowly shrinks toward the center, until eventually (long dashed lines) it drifts out of shape before the run fails around $145M$. Note that the proper area changes linearly and only on the order of 10% during the entire run, see Fig. 1.

Kutta methods). One can obtain these boundary values by interpolation in time, but in a recent paper [30] it is shown that this can lead to a loss of convergence, while the problem does not occur when using a buffer zone of a sufficient number of points. BAM uses three buffer points, and with this prescription our standard evolution method works with FMR out of the box.

Let us summarize our numerical results. For the black hole binary with $\rho_0 = 3.0M$ introduced above, evolution times of up to $185M$ are obtained and a typical run easily exceeds the orbital period of $114M$. Fig. 1 shows the AH

mass for one of the black holes as a function of time. It is important to note that a common AH enclosing both black holes does not form within the achieved evolution time, while for sufficiently small values of ρ_0 (and the same AH finder described in [31] and implemented in Cactus [32]) a common AH is found in [10].

There is an almost linear drift in the AH mass of about 10% per $100M$ at a resolution of $h = M/32$ near the excision region, which becomes smaller with increasing resolution as shown in Fig. 2. Puncture evolutions without excision give a quantitatively very similar result, hence the simple excision technique does not appear responsible for the drift. Since the AH is a slice dependent quantity, the warpage of the slice will contribute to changes in the AH mass. In the future we plan to find event horizons to resolve this ambiguity. Fig. 2 also shows convergence in the AH mass for evolutions of a Schwarzschild black hole in an octant, confirming that our FMR method is convergent. We have also evolved Schwarzschild on quadrants and full grids for $1000M$ and more.

Fig. 3 shows an estimate for the mass at infinity. The errors are satisfactory for the present purpose. Since the AH mass shown in Fig. 1 is not significantly affected by

the location of the outer boundary, we conclude that the interior of the numerical domain has been computed with good accuracy. Fig. 3 also shows the remaining coordinate motion near the black holes. A residual drift of similar magnitude is observed also for larger separations, which is a likely reason for the code failure that occurs after about $150M$ rather independently of separation.

In conclusion, dynamically adjusted commoving coordinates enable us to perform the first numerical simulations of two black holes near but outside the ISCO for about one orbital period. A good indicator for one orbit would be the presence of two cycles of gravitational waves. First experiments with wave extraction indicate that further improvements of the outer boundary are needed.

It is a pleasure to thank M. Alcubierre, A. Ashtekar, N. Dorband, S. Hawley, P. Laguna, D. Pollney, and E. Seidel for discussions. We thank B. Lacki for help with HDF5. We acknowledge the support of the Center for Gravitational Wave Physics funded by the National Science Foundation under Cooperative Agreement PHY-01-14375. This work was also supported by NSF grant PHY-02-18750, and by The Pennsylvania State University.

-
- [1] K. Thorne, *Rev. Mod. Phys.* **52**, 285 (1980).
 - [2] B. Schutz, *Class. Quantum Grav.* **16**, A131 (1999).
 - [3] P. Anninos, K. Camarda, J. Massó, E. Seidel, W.-M. Suen, and J. Towns, *Phys. Rev. D* **52**, 2059 (1995).
 - [4] B. Brügmann, *Int. J. Mod. Phys. D* **8**, 85 (1999).
 - [5] S. Brandt, R. Correll, R. Gómez, M. F. Huq, P. Laguna, L. Lehner, P. Marronetti, R. A. Matzner, D. Neilsen, J. Pullin, et al., *Phys. Rev. Lett.* **85**, 5496 (2000).
 - [6] M. Alcubierre, W. Bengert, B. Brügmann, G. Lanfermann, L. Nerger, E. Seidel, and R. Takahashi, *Phys. Rev. Lett.* **87**, 271103 (2001), gr-qc/0012079.
 - [7] J. Baker, B. Brügmann, M. Campanelli, C. O. Lousto, and R. Takahashi, *Phys. Rev. Lett.* **87**, 121103 (2001), gr-qc/0102037.
 - [8] J. Baker, B. Brügmann, M. Campanelli, and C. O. Lousto, *Class. Quantum Grav.* **17**, L149 (2000).
 - [9] J. Baker, M. Campanelli, C. O. Lousto, and R. Takahashi, *Phys. Rev. D* **65**, 124012 (2002), astro-ph/0202469.
 - [10] M. Alcubierre, B. Brügmann, P. Diener, F. S. Guzmán, I. Hawke, S. Hawley, F. Herrmann, M. Koppitz, D. Pollney, and E. Seidel (2003), in preparation.
 - [11] S. Brandt and B. Brügmann, *Phys. Rev. Lett.* **78**, 3606 (1997).
 - [12] W. Tichy and B. Brügmann (2003), gr-qc/0307027, accepted for publication by *Phys. Rev. D*.
 - [13] W. Tichy, B. Brügmann, and P. Laguna, *Phys. Rev. D* **68**, 064008 (2003), gr-qc/0306020.
 - [14] T. Damour, E. Gourgoulhon, and P. Grandclement, *Phys. Rev. D* **66**, 024007 (2002), gr-qc/0204011.
 - [15] G. B. Cook, *Phys. Rev. D* **50**, 5025 (1994).
 - [16] T. W. Baumgarte, *Phys. Rev. D* **62**, 024018 (2000), gr-qc/0004050.
 - [17] M. Alcubierre, B. Brügmann, P. Diener, M. Koppitz, D. Pollney, E. Seidel, and R. Takahashi, *Phys. Rev. D* **67**, 084023 (2003), gr-qc/0206072.
 - [18] M. Alcubierre and B. Brügmann, *Phys. Rev. D* **63**, 104006 (2001), gr-qc/0008067.
 - [19] M. Alcubierre, B. Brügmann, D. Pollney, E. Seidel, and R. Takahashi, *Phys. Rev. D* **64**, 61501 (R) (2001), gr-qc/0104020.
 - [20] U. Sperhake, K. L. Smith, B. Kelly, P. Laguna, and D. Shoemaker (2003), gr-qc/0307015.
 - [21] B. Brügmann, in preparation.
 - [22] M. W. Choptuik, *Phys. Rev. Lett.* **70**, 9 (1993).
 - [23] T. Plewa, <http://flash.uchicago.edu/~tomek/amr>.
 - [24] P. Diener, N. Jansen, A. Khokhlov, and I. Novikov, *Class. Quantum Grav.* **17**, 435 (2000), gr-qc/9905079.
 - [25] D.-I. Choi, J. D. Brown, B. Imbiriba, J. Centrella, and P. MacNeice (2003), physics/0307036.
 - [26] M. W. Choptuik, E. W. Hirschmann, S. L. Liebling, and F. Pretorius, *Phys. Rev. D* **68**, 044007 (2003), gr-qc/0305003.
 - [27] F. Pretorius and L. Lehner (2003), gr-qc/0302003.
 - [28] B. Brügmann, *Phys. Rev. D* **54**, 7361 (1996).
 - [29] G. Lanfermann, Master's thesis, Freie Universität Berlin, MPI für Gravitationsphysik (1999).
 - [30] E. Schnetter, S. H. Hawley, and I. Hawke (2003), gr-qc/0310042.
 - [31] M. Alcubierre, S. Brandt, B. Brügmann, C. Gundlach, J. Massó, E. Seidel, and P. Walker, *Class. Quantum Grav.* **17**, 2159 (2000), gr-qc/9809004.
 - [32] Cactus, <http://www.cactuscode.org>.